Failure of an Earthen Dam and Its Possible Strengthening Methods

Bhuddarak CHARATPANGOON[1], Junji KIYONO[2], Aiko FURUKAWA[3] and Chayanon HANSAPINYO[4]

[1]Dept. of Urban Management, Kyoto University
(Kyoto daigaku-katsura, Nishikyo-ku, Kyoto 615-8530, Japan)
E-mail:bhuddarak@hotmail.com
[2]Member of JSCE, Professor, Graduate School of Global Environmental Studies, Kyoto University
(Kyoto daigaku-katsura, Nishikyo-ku, Kyoto 615-8530, Japan)
E-mail: kiyono.junji.5x@kyoto-u.ac.jp
[3]Member of JSCE, Associate Professor, Graduate School of Global Environmental Studies, Kyoto University
(Kyoto daigaku-katsura, Nishikyo-ku, Kyoto 615-8530, Japan)
E-mail: furukawa.aiko.3w@kyoto-u.ac.jp
[4]Assistant Professor, Dept. of Civil Engineering, Chiang Mai University
(239 Huay Kaew Road, Muang District, Chiang Mai 50200, Thailand)
E-mail: chayanon@eng.cmu.ac.th

This study aimed to examine the failure mechanisms of the Fujinuma dam and introduce possible seismic strengthening methods for earth dam. The study comprises of field and laboratory experiments, and a numerical simulation of the dam. Laboratory experiments were conducted to acquire necessary information. For the seismic analysis, a coupled solid-fluid finite element formulation was applied. The observed and simulated motions of the 2011 Tohoku Earthquake used as input motions. Frequency and dynamic analyses were performed thereafter dam behavior and possible failure mechanisms were presented. Besides, the seismic stengthening techniques of the studied dam have been introduced and therefore discussed.

Key Words : *earthen dam, dam failure, seismic safet , finite element, strengthening method*

1. INTRODUCTION

Following the devastating earthquake in Japan on 11 March 2011, seven dams were damaged and the Fujinuma dam collapsed owing to the 9.0-magnitude earthquake, known as the 2011 Off the Pacific Coast of Tohoku Earthquake (hereafter, the 2011 Tohoku earthquake). The Fujinuma dam was constructed to serve as a water supply for irrigation purposes. The dam was failed following the 2011 Tohoku earthquake. The failure caused a flood that washed away houses and damaged others, disabled a bridge, and blocked roads with debris. Therefore, to assure dam safety, proper evaluation of such dams is crucial. Accordingly, the failure of the Fujinuma dam can be regarded as a fruitful resource which provided a better understanding on the dam failure mechanisms and to acquire useful information relating to seismic safety of an earth dam.

Recently, as advanced computational techniques in geotechnics have been introduced, it has become beneficial for researchers[1)-4)] to analyze seismic behavior of dams by using those techniques. Consequently, much research has been conducted in the area of seismic safety on existing earth dam. All of these methods have been applied to evaluate the safety of earth dam. The importance of such research is not only to examine the behavior of a dam or the level of damage it can sustain, but also to preserve it against future earthquakes.

Since, the knowledge on the earthquake engineering have been well established, concerned groups are now raising the awareness on the safety of their structures including dam. Therefore, many researchers[5)-7)] proposed the seismic strengthening methods for embankment dam such as adding downstream berms, increasing freeboard, enlarging a dam, replacing improper soil, enhancing drainage system, establishing an emergency action plan or even considering for no action. The suggestion and discussion for each methods were presented. Eventually, the most proper technique has been recommended along with the comparison between other techniques.

Among all, for strengthening soil structure, geogrid is now becoming popular due to its effectiveness. Previous researches[8), 9)] conducted the study on the geogrid reinforced embankment. The results demonstrated that the geogrid could improve the stability of the embankment with comparatively higher than other conventional methods.

This study aims to gain insight into the behavior of the Fujinuma dam during the time of the earthquake by using the Finite element (hereafter, FE) method. Both the observed and simulated motions were used to determine the response of the dam during the excitation. The soil behavior of the dam materials is described by using the Mohr-Coulomb soil model available in the Plaxis FE code[10)]. Dynamic analyses of the model are conducted, and the overall dam behaviors are presented. Discussions and comparisons between the simulation results and existing facts are expressed. Also, the seismic strengthening techniques are introduced as the alternative methods for improving the seismic safety of an earth dam and the results are therefore discussed.

2. DAM SITE AND INPUT MOTIONS

(1) Fujinuma dam and input motions

Fujinuma dam was an earth-fill embankment dam near Sukagawa, Fukushima prefecture, Japan. It was established on the Ebana River, a tributary of the Abukuma River, 16 km west of the city office of Sukagawa (37° 18′ 07″ N, 140° 11′ 41″ E). The purpose of the dam was water supply for irrigation. The typical cross section of the main dam is shown in **Fig.1**. The dam was an embankment type, 18.5 m high and 133 m long with a structural volume of 99,000 m^3 and a crest width of 6 m. The dam was at the head of an 8.8-km^2 drainage area giving a reservoir capacity of 1,504,000 m^3[11)].

(2) Dam materials and their properties

In this study, laboratory experiments have been conducted to extract the necessary information for studying the dam failure. Facts and discussions of dam material obtained from laboratory experiments are presented and discussed. To facilitate the numerical simulation and study of the dam failure, thirteen undisturbed cylinder samples were collected at the site. These samples can be defined based on their origin and testing purpose, as shown in **Table 1**.

a) Sieve analysis

Sieve number applied in this study was in the range of 4–200. The results show that both the middle and bottom layer consist of a high percentage of fine particle sizes (**Fig.2**). Furthermore, about 30–40% of the particles in these layers are smaller than 0.1 mm, whereas the upper part is shown to consist mainly of sandy materials. The boundaries for potentially liquefiable soil (b-b) and boundaries for most liquefiable soil (a-a) are shown in **Fig.2**[12)]. Accordingly, it can be determined that the bottom and middle portions were not vulnerable to liquefaction because their distribution curves show high percentages of fine particles. Also, the information on the distribution of fine particles was obtained from the study of Tanaka et al.[13)]. According to their study and laboratory experiment, they have presented that the clay content (particles smaller than 2 μm) of the middle and bottom portions is about 30% and 10%, respectively. Andrews and Martin[14)] summarized that soils are susceptible to liquefaction if they contain less than 10% finer than 2 μm and liquid limit less than 32, soils are not susceptible to liquefaction if they contain greater or equal to 10% finer than 2 μm and liquid limit greater or equal to 32. Accordingly, both the middle and bottom are not susceptible to liquefaction. Moreover, from the site investigation, there is no obvious evidence such as sand boils at the site, to confirm the occurance of the liquefaction.

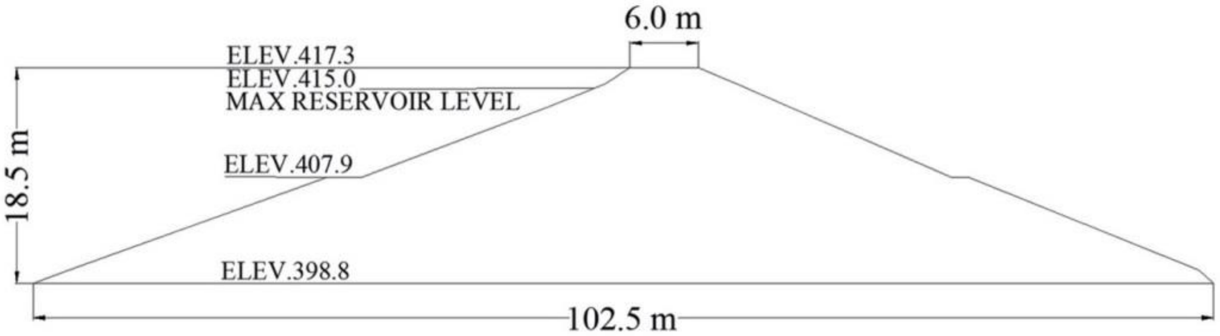

Fig.1 Typical cross section of the main dam

Table 1 Soil samples

Test	Number of samples
Permeability	1
Triaxial CU	12
• Bottom	4
• Middle	4
• Upper	4
Total	13

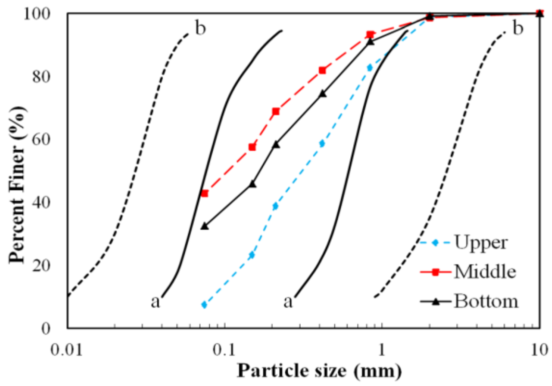

Fig.2 Particle size distribution

Table 2 Material properties

Materials	Layer	γ_{dry} (kN/m^3)	γ_{sat} (kN/m^3)	$k_y \cong k_x/4$ (μm/s)	E (MPa)	K_w/n (GPa)	υ	c' (kPa)	ϕ' (deg)
Dam body	Bottom	16.0	18.0	0.55	50.0	1.87	0.30	18.4	31.0
	Middle	14.0	16.0	0.55	30.0	1.12	0.30	7.80	32.0
	Upper	16.0	18.0	0.55	17.5	0.65	0.30	0.00	37.0
Foundation		30.0	-	-	300	-	0.20	-	-
Geogrid	Axial stiffness, EA (MN/m)				Tensile strength (kN/m)				
	10.0				200				

b) Triaxial test

In order to get material properties for conducting FE analysis of the dam, the consolidated–undrained triaxial test was applied in this study, therefore. The triaxial test results are presented in **Table 2**. The dry γ_{dry} and saturated unit weight γ_{sat} defined the mass for the element located in dry and saturated areas, respectively. Permeability or hydraulic conductivity k described the fluid movement through porous media. In the elastic range, the modulus of elasticity E indicated the relationship between stress and strain within the elastic region, and Poisson's ratio υ provided information on the effect of the load in one direction in relation to the deformation in other directions. The shear strength parameters cohesion c and friction angle ϕ were used to form the failure surface for this model. Finally, by considering slight compressibility of water, the rate of excess pore pressure was defined as Kw/n, in which Kw is the bulk modulus of water and n is the soil porosity. For geogrid properties were obtained from previous researchers[8), 9)]. The geogrid parameters were defined only in term of axial rigidity, EA and tensile strength.

(3) Input motions

Regards to the 2011 magnitude 9.0 (Mw) undersea megathrust earthquake off the Pacific coast of Japan (JMA) [15)], which occurred on 11 March 2011, two motions were selected for using as input motions in this study; the first one is the ground motion record obtained from Station FKS017, Sukagawa, Fukushima, Japan, was provided by the Kyoshin network and operated by the National Research Institute for Earth Science and Disaster Prevention[16)]. These data were observed about 15 km away from the site; And also, another motion was from obtained Hata et al. [17)]. They estimated the simulated ground motion for the dam site by microtremor observation by using the site effect substitution method. The peak ground acceleration amax was 4.198 and 4.25 m/s^2 for the observed and simulated motions, respectively (**Fig. 3a** and **b**). The spectra of both motions are shown in **Fig.3c** and **d**. The predominant period of both motions was 2.71 and 2.96 Hz, respectively. The smoothed spectra of both motions were also introduced by applying a 50-period moving average (50 per.Mov.Avg.).

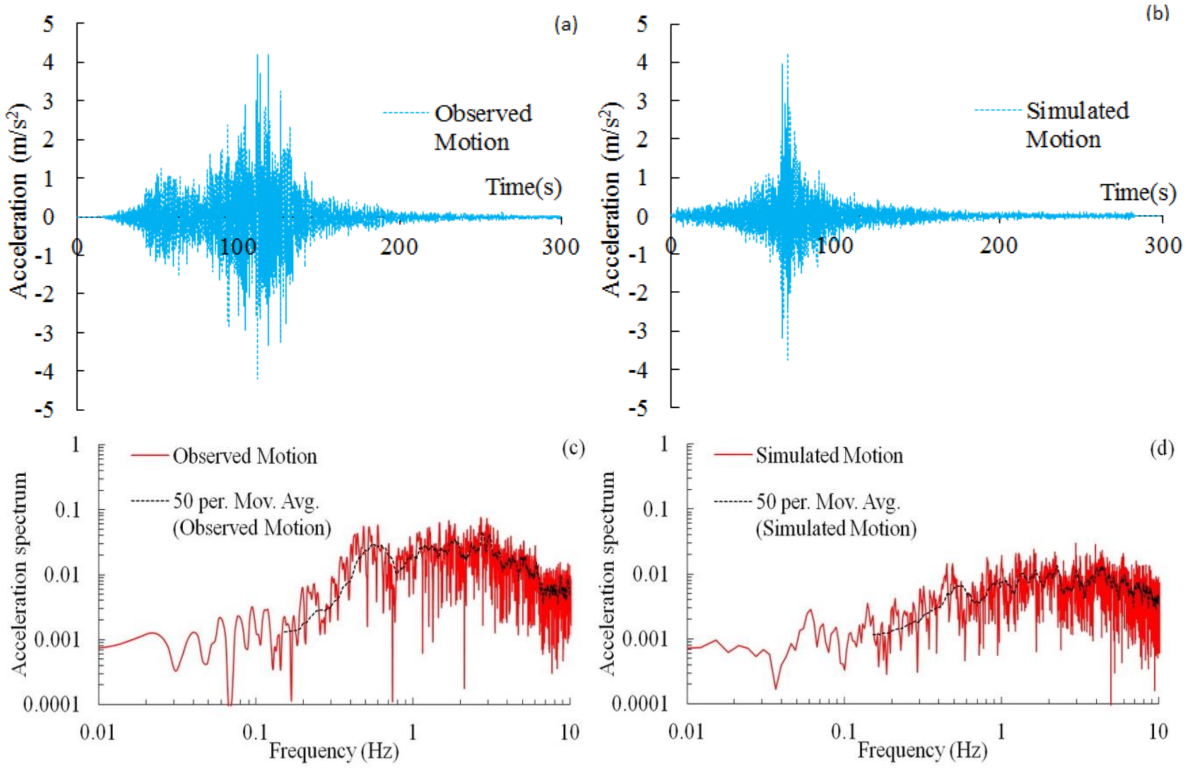

Fig.3 Input motions. (a) Observed motion at FKS017 15 km from the dam site. (b) Simulated motion at the dam site. (c) Spectrum of observed motion. (d) Spectrum of simulated motion.

3. METHODOLOGY

(1) FE model

The FE analysis was performed under plane strain conditions. The effect between the solid and fluid phase was carried out using a u-p formulation. In this study, triangular 15-noded element with three-point Gaussian integration, a second-order polynomial interpolation for the displacements, and a first-order interpolation for the pore water pressure were used. For the failure analyses of the dam, two dam models have been proposed for this study. The first model represents the original shape of the typical section of the Fujinuma dam (**Fig.4**), and the latter is based on the remaining cross section of the failed dam with regard to the site investigation (**Fig.5**). The first model (hereafter, the actual dam model) was used for conducting dynamic analyses to study on the dynamic behavior and failure mechanism. The second dam model (hereafter, the remaining dam model) was used to determine the dam's mode shapes and their corresponding natural frequencies, and to verify with the microtremor observation results. The foundation was modeled by extending a 10-m-thick layer 100 m either side of the center. The boundary conditions were restrained in the horizontal and vertical directions at the bottom of the model. For both edges, the boundary conditions were fixed only in the lateral direction and were free in the vertical direction. The dam's body was classified into three portions: upper, middle, and bottom. Dynamic analysis was performed using the Plaxis FE code[10]. Rayleigh damping was assumed in the dynamic analysis by considering 5% damping in the frequency range of 1.64–2.45 Hz.

For studying the possible strengthening method, there are three methods were proposed and analyzed to find out the proper solutions for the studied dam. In dynamic analysis of these strengthening models, only simulated motion was used as input motion because it is quite difficult to compare each methods when using the vigorous observed motion. The strengthening techniques presented in this study are as the followings; 1) adding berm to the downstream slope by the half of the dam's height (hereafter, S1). S1 model is shown in **Fig.6**. For S1, the amount of the added soil volume was about 20% of the actual dam volume and its properties were considered to be the same as the middle soil layer used in the original dam body; 2) enlarge dam by increasing dam height and adding downstream berm (hereafter, S2). S2 model is shown in **Fig.7**. The actual dam was enlarged by increasing crest height by 4.0 m, doubling the crest width and also adding downstream berm

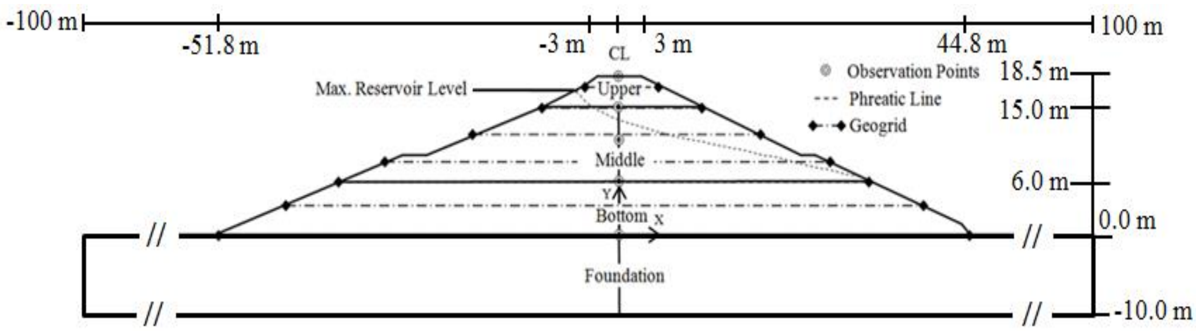

Fig.4 Actual dam model and Strengthening model 3, S3

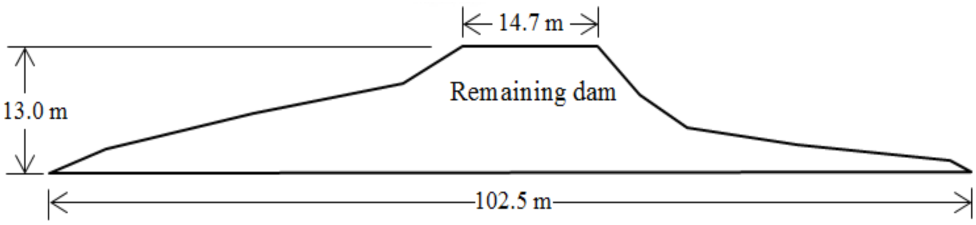

Fig.5 Remaining dam model

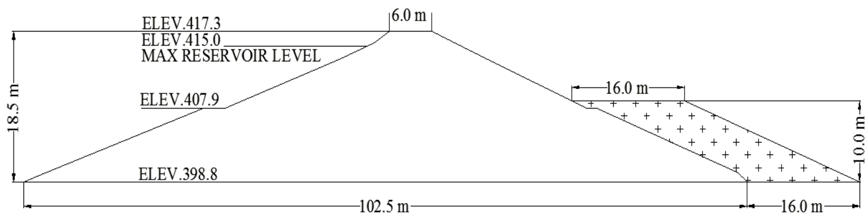

Fig.6 Strengthening model 1, S1

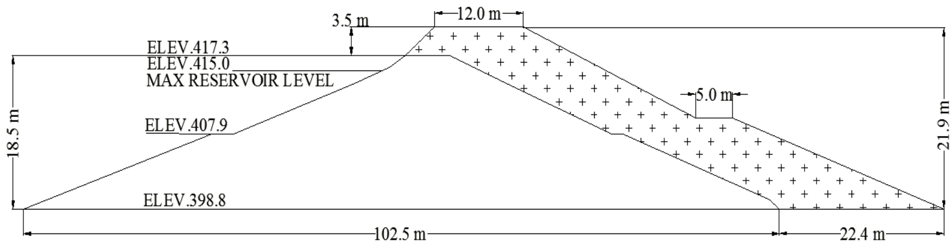

Fig.7 Strengthening model 2, S2

which total added soil volume was about 40% of the original dam volume; 3) geogrid reinforced dam (hereafter, S3), some modifications were made. Geogrids were applied in the dam body with 3 m spacing between each layer form the bottom to the crest that resulting in a total of 7 geogrid layers (Fig. 4). The geogrid was modeled as a cable element which is considered only the axial rigidity and can only resist tensile force. In all strengthening models, the upper portion of the dam were replaced by the material that applied in the middle portion of the dam which considered as one of the strengthening methods for this dam.

As the purpose of this study is to determine the failure mechanisms of the Fujinuma dam and to introduce its possible strengthening techniques. Therefore, the analysis can be divided into two parts; first, the actual and remaining dam models were analyzed to study on the dynamic behavior and its failure; and the dynamic analyses of all strengthening models were conducted. The results for all cases were then discussed and compared.

(2) Constitutive law

The behavior of the dam materials is described using the Mohr-Coulomb soil model, which is an elastic–perfectly plastic model with a yield surface whose elastic behavior is defined by isotropic elasticity through a linear Young's modulus *E*. The model has yield surfaces defined by cohesion *c* and friction angle ϕ. The generalization of the Coulomb friction failure law is then defined by

$$\tau = \sigma_n \tan\phi + c \qquad (1)$$

In which τ is the magnitude of the shearing stress, σ_n is the normal stress, c is cohesion, and ϕ is the angle of internal friction. The parameters of the dam material were obtained mainly from the laboratory experiments, as mentioned earlier in relation to **Table 2**, whereas the properties of the foundation and geogrid were assumed. Each parameter used in the analysis was described as mentioned earlier.

4. RESULTS AND DISCUSSIONS

(1) Modal analysis

Modal analysis is conducted to extract the natural frequency and its corresponding mode shape. In this study, two dam models were analyzed. Both cases were analyzed under the empty reservoir condition. For the actual dam model, the natural frequency is 1.64 and 2.45 Hz for the first two modes, respectively. For the remaining dam model, the natural frequency is 2.35 Hz for the translational mode in the horizontal direction.

Fig.8 shows the amplification ratio that was taken from the top of the remaining dam to two locations

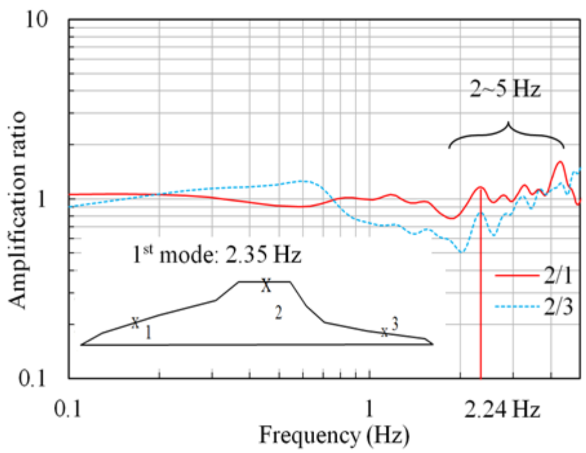

Fig.8 Amplification ratio

Table 3 Modal anlysis results

Model	Actual	S1	S2	S3
1st Mode	1.64 Hz	1.76 Hz	1.40 Hz	1.77 Hz
Direction	Horizontal			
2nd Mode	2.45 Hz	2.61 Hz	2.14 Hz	2.65 Hz
Direction	Vertical			

near the dam base of the upstream and downstream slopes, defined as 2/1 and 2/3, respectively. By comparing the numerical results with microtremor test results, it can be seen that in the latitudinal direction, the amplification ratio is within the range of 2–5 Hz. The results obtained from the modal analysis of the remaining dam agree well with field observations in relation to the vibration in the latitudinal direction. Therefore, the estimated predominant frequencies of the original dam are 1.64 and 2.45 Hz. Besides, the natural frequency of all strengthening dam models is therefore 1.76–2.61 Hz, , 1.40–2.14 Hz and 1.77–2.65 Hz, respectively. The summaries of all proposed models were shown in **Table 3**.

(2) Dynamic analysis

A dynamic analysis is performed to determine the possible behavior of the dam during an earthquake. The results were expressed through acceleration, deformation and shear strain.

a) Acceleration

The maximum crest acceleration is determined to be 7.42 m/s^2 and 7.60 m/s^2 accelerating towards the upstream direction at the time of 104.45s and 72.78 s for the observed and simulated motions, respectively. For both cases, it can be seen that the crest acceleration is amplified significantly. The maximum amplification ratio taken from the crest to the base is 1.76 and 1.79 for both motions, respectively.

The observed motion contains high-amplitude waves for a longer duration than does the simulated motion. This generates a great response throughout the dam body resulting from significant inertial force acting on the dam. This causes a great amount of plastic deformation and eventually the dam failure owing to the loss of freeboard. In contrast, the simulated motion contains high-amplitude waves only for a comparatively short period; thus, this does not contribute a sufficient effect to cause large movement and settlement of the dam.

For the strengthening models, all cases were analyzed by using the simulated motion. The summaries of the crest acceleration with its direction and the maximum crest to base amplification ratio were shown in **Table 4**. The results showed that the maximum crest acceleration can be seen from the S1 which is determined to be 9.63 m/s^2 accelerating towards the upstream direction. Whilst, the lowest maximum crest acceleration belongs to the S3 that is about 8.48 m/s^2 acting toward the upstream side. For all cases, it can be seen that the crest acceleration is amplified obviously. The highest maximum amplification ratio taken from the crest to the base is 2.20

while the lowest is 2.0 using S1 and S3, respectively.

The results show that the actual dam model is less sensitive to the excitation than the reinforced dam models. This is due to the higher rigidity provided in the retrofit models and also the actual model could easily displace and dissipate the energy from the earthquake excitation.

Table 4 Acceleration

Model	Actual	S1	S2	S3
Crest Acceleration (m/s^2)	7.60	9.63	8.80	8.48
Direction (Upstream, U) (Downstream, D)	U	U	D	U
Amplification ratio	1.79	2.20	2.05	2.0

b) Deformation

Deformation can be used as an index for judging the safety of the dam due to freeboard loss. The results are expressed through the crest displacement during the excitation.

Fig.9 shows the deformed mesh at 104.19 s and its corresponding displacement curves when subjected to the observed motion. It can be seen that the entire dam body was moved in the downstream direction. As time increases, plastic deformations were accumulated. This caused the permanent horizontal displacement Ux of 2.95 m, and crest settlement Uy reached 1.80 m at 104.19 s; this is considered as the point of dam failure due to the loss of freeboard. Settlements at other observation points yield a similar tendency, but the settlements were less with decreasing dam height.

Deformation in both directions at the end of the shaking using simulated motion and the actual dam model was 0.30 m and 0.65 m for the horizontal displacement and crest's settlement, respectively.

In case of strengthening models, the permanent horizontal displacement at the dam crest was 0.57, 0.005 and 0.47 m for the strengthening model 1 to 3, respectively. And, the settlement at the dam crest obtained using the strengthening model 1 to 3, was 0.49, 0.19 and 0.39 m, respectively. As a result, by considering overtopping failure, all models were able to withstand safely the simulated motion. However, due to uncertainty in the numerical analysis and the material model together with the previous study on the performance of a fill dam based on the performance based design concept[7] suggested that the safety factor of 2.0 should be taken into account. Accordingly, it is recommended that the settlement of the crest should not exceed 1.0 m so the allowable settlement should be limited at 0.5 m. Therefore, all retrofit cases are able to satisfy this criterion.

According to the facts, the dam experienced overflow and subsequent to the dam breach. The one possible cause is that the significant settlement of the dam body led to the loss of freeboard. Although, the results obtained from actual dam model were not cause the loss of freeboard, the settlement is high, especially in the upper portion of the dam owing to its softness.

The summaries of deformation using all models were shown in **Table 5**. By comparing the actual dam model and the strengthening models, it can be summarized that the minimum crest settlement was obtained from the S2 which is 70.1% dropped from the actual model.

c) Shear strain

Shear strain provides information for under-

Table 5 Deformation

Model		Actual	S1	S2	S3
Crest Deformation (m)					
Direction	Ux	0.30	0.57	0.005	0.47
	Uy	-0.65	-0.49	-0.19	-0.39
% different	Ux	-	90.4	98.3	38.3
	Uy	-	24.2	70.1	53.7

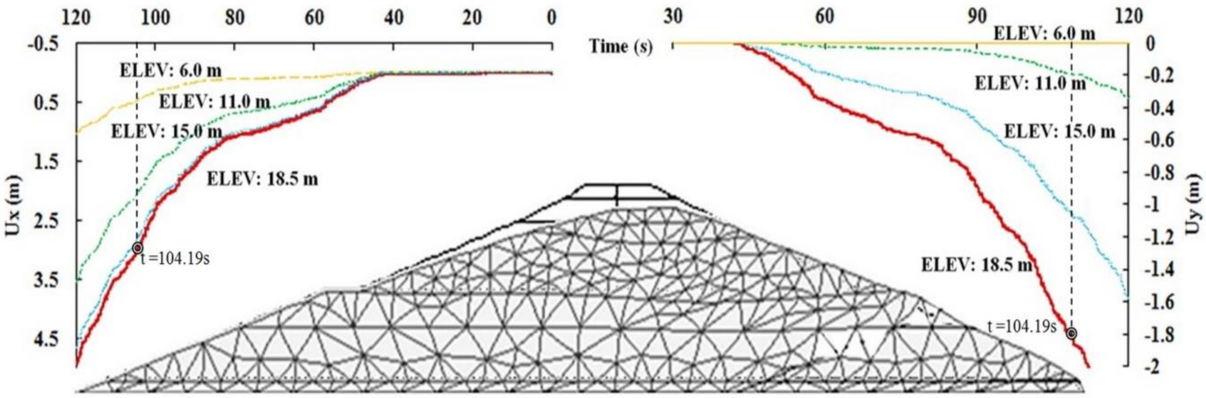

Fig.9 Actual dam model

standing the location within the dam body that might be damaged severely during the earthquake excitation.

Shear strain contours of the actual dam model when subjected to the simulated motion at various times is shown in **Fig.10**. For both motions, similar trend can be observed. Most of the dam body experienced an insignificant rate of shear strain. It can be seen that initially, large shear strains occurred in the upper portion, especially on the upstream side. Thereafter, the occurrences of large shear strain can be observed clearly on both sides of the dam in the middle and bottom portions of the downstream slope. This excessive level of shear strain may indicate a possible cause for the dam failure.

Similarly, the sequence of dam failure has been reported by previous researchers[13), 18), 19)] indicated that initially the dam experienced excessive deformation or a slide on the upper portion of the upstream slope. This, together with a subsequent large slide that occurred on the downstream face, yielded a loss of freeboard and triggered the overflow that resulted in the breaching of the dam. Therefore, it can be seen that the numerical results show good agreement with this scenario.

Shear strain contours at the end of the excitation obtained from the strengthening model S1 and S2 are shown in **Fig.11**. Also, Shear strain contours of S3 for various times were shown in **Fig.12**. Similarly, the same trend can be seen in all strengthening models but in smaller values and shear strain at the top portion appear to be vanished. By comparing the actual dam model with all strengthening models, it can be drawn that the maximum value of shear strain obtained from strengthening dam models were greatly dropped by using S2 and S3. Therefore, Some of the proposed methods are seem to be an effective measure for strengthening this structure especially it could solve a problem on the large shear strain at the top portion effectively.

5. CONCLUSIONS

This study aimed to understand the dynamic behavior and the possible failure mechanism of the earth dam. As the Fujinuma dam was failed after the 2011 Tohoku earthquake, it was then selected for using as a model in this study. The study of the fujinuma dam includes the dynamic behaviors, failure mechanism and also its possible strengthening methods.

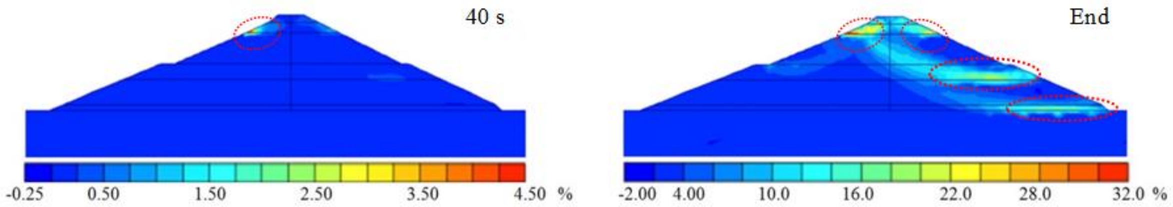

Fig.10 Shear strain contours at 40 s and at the end of motion using the simulated motion (actual dam model)

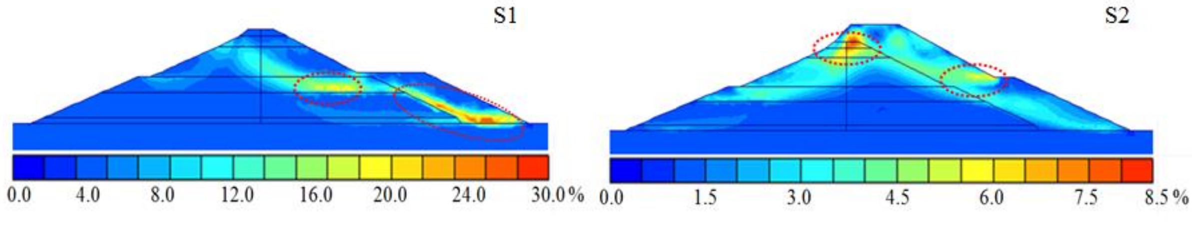

(a) (b)

Fig.11 Shear strain contours at the end of motion using the simulated motion. (a) S1. (b) S2.

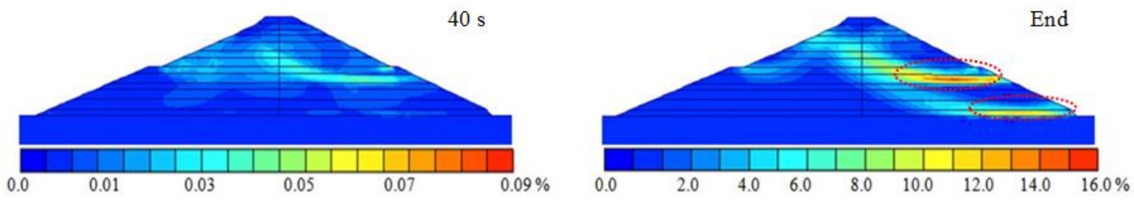

Fig.12 Shear strain contours at 40 s and at the end of motion using the simulated motion (S3)

In this study, the microtremor observations were conducted to find out the natural frequency of the original dam and also the remaining portion of the dam. By considering the application ratio taking at crest to base, it can be seen that the natural frequency of the remaining dam obtained from numerical simulation showed a good agreement with the microtremor test results. Therefore, the same analysis's parameters were used for determining the natural frequency of the actual dam model.

The dynamic analysis results of the actual dam model when subjected to the observed motion showed that the entire dam body was moved in the downstream direction and large plastic deformations were accumulated. This caused crest settlement reached 1.80 m at 104.19 s which is considered as the point of dam failure due to the loss of freeboard. In case of using simulated motion, the settlement of the dam crest was 0.65 m. By considering the availably of freeboard length, the dam seems to be safely withstanding the simulated motion. However, due to uncertainty in the numerical analysis and the material properties, previous researchers[7)] suggested that the safety factor of 2.0 should be taken into account. Therefore, according to the performance based of a fill dam, it is recommended that the settlement of the crest should not exceed 1.0 m so the allowable settlement should be limited at 0.5 m. Therefore, the actual dam model is not able to satisfy this criterion.

According to the numerical result of the actual dam model, it can be summarized that the model experienced large shear strains. The large shear strains were observed initially in the upper portion of the upstream slope, following which large shear strains commenced on the downstream side. These, together with tension cracks, might evidently indicate the cause of the sliding failure of the dam slope and might possibly trigger the overtopping of the dam. In addition, these sliding patterns exhibit good agreement with the facts gathered from field observations.

There are three strengthening techniques have been introduced in this study. Those methods were proposed in order to find out the suitable mitigation for strengthening the existing dam that could possibly be applied in the similar cases in future for preventing the dam from its failure. These strengthening methods are; 1) S1, added downstream berm by half of the dam's height; 2) S2, enlarged and increased dam height; 3) S3, applied geogrid reinforcement layers. All strengthening models were analyzed using the simulated motion because it is difficult to compare the results using the observed motion.

The results clearly indicated that S2, S3 are seem to be effective measures for reducing the risk of failure of this studied dam. Above all, the S2 found to be most effective way for strengthening the studied dam especially in case of existing dam due to its simplicity and also the crest settlement found to be smallest among other techniques. By raising the dam height and adding downstream berm, these together made this strengthening method could safely resist the simulated motion. S3 or geogrid reinforced model found also to be a good measure as it could reduce the crest settlement as well as the shear strain which is much smaller than that observed in the actual dam model. However, in case of the existing dam, S2 found to be more appropriate as it is quite simply to construct while the geogrid reinforcement seems to be suitable for new constructing dam.

Most strengthening techniques proposed herein this study were mainly focused on the structural content. Yet, the best solution needs to take into account of many factors like; workability, economy and the important of the dam, effect to downstream site, for selecting the most suitable method for each case. Therefore, where compromised between the strengthening method, cost and the accepted damage level could be met, other measures such as early planning, establishing inundate map and making evacuation plan or even "no action" might considered to be possible mitigation for this dam as well.

Through this study, it can be seen that there is always a risk for those people who lived near the dam site especially at downstream side. The Fujinuma dam was an existing dam which constructed in the past when the modern seismic design was not yet established. Also, the seismic safety evaluation of this dam using the state of the art techniques was not conducted. In fact, this study presented only one case, there are still numerous of existing fill dams were needed to be evaluate their seismic safety to ensure the safety of people and their properties. Therefore, the seismic safety evaluation of existing dams is crucial and indeed urgent. Otherwise, when future quake strikes it might bring about a disaster to those who live downstream. Thus, this study demonstrates that it is very important not only to design a dam that is capable of withstanding future quakes, but the investigation, maintenance and mitigation of existing dams are vital for seismic safety of dam.

ACKNOWLEDGMENT: The authors would like to acknowledge the contributions of the National Research Institute for Earth Science and Disaster

Prevention for providing invaluable information. Special thanks are extended to Dr. Yoshiya Hata, Prof. Susumu Nakamura, and Dr. Atsushi Nozu for providing the ground motion used in this study. The authors would also like to thanks both Prof. Mamoru Mimura, Prof. Susumu Iai and staffs of the laboratory of Geo-disaster Division, Disaster Prevention Research Institute, Kyoto University, Japan, for their help in handling the instruments. The authors would also like to express their great appreciation to Dr. Suttisak Soralump from Kasetsart University for his useful and constructive suggestions during the site observation.

REFERENCES

1) Woodward, P. K. and Griffiths, D. V. : Influence of viscous damping in the dynamic analysis of an earth dam using simple constitutive models, *J. Computers and Geotechnics.*, Vol. 19, No. 3, pp. 245-263, 1995.
2) Li, C., Borja, R. I. and Regueiro, R. A. : Dynamics of porous media at finite strain, *Computation Methods in Applied Mechanics and Engineering*, Vol. 193, pp. 3837-3870, 2004.
3) Rampello, S., Cascone, E. and Grosso, N. : Evaluation of the seismic response of a homogeneous earth dam, *J. Soil Dynamics and Earthquake Engineering*, Vol. 29 ,pp. 782-798, 2009.
4) Fallah, H. and Wieland, M. : Evaluation of Earthquake Safety of Koman Concrete Face Rockfill Dam in Albania, *Proc. of 3rd Asian Conference on the Earthquake Engineering, ACEE*, Bangkok, Thailand, 2010.
5) Perlea, V., Mathews, D. and Empson, W. : Evaluation of alternatives for earthquake hazard mitigation of an embankment dam in Kansas, *Proc. of 13th world conference on earthquake engineering*, Vancouver, B.C., Canada, August 1-6 paper number 1895, 2004.
6) Fade, M., Yazdani, M. and Azad, A. : Seismic retrofit of embankment dams based on dynamic nonlinear analyses, *Proc. of 12th international conference of international association for computer methods and advances in geomechanics(IACMAG)*, October 1-6, Goa, India, 2008.
7) Tani, S., Tsukuni, S. and Shiomi, T. : Performance of a fill dam based on the performance-based design concept and study of a seismic retrofitting method, *J. Soils and foundations*, Vol. 49, No. 6, pp. 841-851, 2009.
8) Wulandari, P. S. and Tjandra, D. : Determination of optimum tensile strength of geogrid reinforced embankment, *Proc. of International Civil Engineering Conference "Towards Sustainable Civil Engineering Practice"*, Surabaya, August 25-26, 2006.
9) Moradi, G., Abdolmaleki, A., Ahmadvand, M. and Ghadami, H. : Stabilization of rock slopes using geosynthetic materials as new approach and its comparison with conventional methods, *Proc. of International symposium on advances in science and technology*, Bandar-abbas, Iran, 2013.
10) Brinkgreve , R. B. J. and Vermeer, P. A. : *Plaxis ver. 7, Material models manual*, Balkema, Rotterdam, 1998.
11) Wikipedia. [Online]. Available: /http://en.wikipedia.org /wiki/Fujinuma_Dam. [accessed 07/01/12]
12) Japan port and Harbor Association. : *Technical standards for port and harbor facilities in Japan*, pp. 281-288, 1999.
13) Tanaka, T., Tatsuoka, F., Mohri, Y. : Earthquake Induced failure of Fujinuma Dam, *Proc. of International symposium on dams for a changing world, ICOLD*, Kyoto, Japan, Vol. 6, pp. 47-52. 2012.
14) Andrews, D. C. A. and Martin, G. R. : Criteria for liquefaction of silty soils, *Proc. of the 12th World Conference on Earthquake Engineering*, New Zealand, 2000.
15) Japan Meteorological Agency (JMA). [Online]. Available: /http://www.jma.go.jp/en/quake/ [accessed 06.07.12]
16) National Research Institute for Earth Science and Disaster Prevention (NIED). [Online]. Available: /http://www.kyoshin.bosai.go.jp. [accessed 06.01.12]
17) Hata, Y., Nakamura, S. and Nozu, A. : Seismic waveform evaluation at the Fujinuma Dam for the 2011 off the Pacific coast of Tohoku Earthquake-Application of site effect substitution method to a huge subduction earthquake, *J. Structural Engineering, Vol. 58A, JSCE* , pp. 250-263, 2011.
18) Harder, L. F. Jr., Kelson, K. I., Kishida, T., Kayen, R. : Preliminary Observations of the Fujinuma dam failure following the March 11, 2011 Tohoku Offshore Earthquake, Japan, *Geotechnical reconnaissance of the 2011 Tohoku Japan Earthquake, GEER Association 25e*, 2011.
19) Ono, K., Kazama, S., Kawagoe, S., Yokoo, Y., Gunawardhana, L. : Possible earthen dam failure mechanisms of Fujinuma reservoir due to the Great East Japan Earthquake of 2011, *Hydrological Research Letters 5 (2011)*, pp. 69-72, 2011.